

RSC Advances



This is an *Accepted Manuscript*, which has been through the Royal Society of Chemistry peer review process and has been accepted for publication.

Accepted Manuscripts are published online shortly after acceptance, before technical editing, formatting and proof reading. Using this free service, authors can make their results available to the community, in citable form, before we publish the edited article. This *Accepted Manuscript* will be replaced by the edited, formatted and paginated article as soon as this is available.

You can find more information about *Accepted Manuscripts* in the [Information for Authors](#).

Please note that technical editing may introduce minor changes to the text and/or graphics, which may alter content. The journal's standard [Terms & Conditions](#) and the [Ethical guidelines](#) still apply. In no event shall the Royal Society of Chemistry be held responsible for any errors or omissions in this *Accepted Manuscript* or any consequences arising from the use of any information it contains.

1 **Novel magnetic lignin composite sorbent for chromium(VI)**
2 **adsorption**

3 **Zhanxin Song, Wei Li, Wentao Liu, Yan Yang, Ningning Wang, Haijun Wang*,**
4 **Haiyan Gao**

5 *The Key Laboratory of Food Colloids and Biotechnology, Ministry of*
6 *Education, School of Chemical and Material Engineering, Jiangnan University, Wuxi*
7 *214122, China*

8

9

10

11 **Corresponding author:** Haijun Wang

12 **Address:** School of Chemical and Material Engineering, Jiangnan University, Wuxi,
13 Jiangsu, 214122, China

14 **Email:** wanghj329@outlook.com (H.-J. Wang)

15 **Abstract:** A novel magnetic lignin composite was prepared and modified with
16 diethylenetriamine. The properties of the composite were characterized by SEM,
17 FTIR, XRD, TGA and VSM. Then, the adsorption of chromium(VI) from aqueous
18 solutions using this magnetic lignin composite was investigated. Chromium(VI)
19 removal is pH dependent and the optimum adsorption was observed at pH 2.0. The
20 pseudo-second-order model and the Langmuir adsorption isotherm model were
21 applied to describe the adsorption kinetics and adsorption isotherm, respectively, for
22 the chromium(VI) adsorption. Thermodynamic parameters were calculated, which
23 revealed the adsorption process to be spontaneous and exothermic. Regeneration of
24 the magnetic lignin composite was achieved by using 0.4M NaCl and 0.2 M NaOH,
25 more than 87% efficiency retention was obtained after 5 cycles.

26 **Keywords:** Magnetic lignin composite; Adsorption; Chromium(VI)

27

28 1. Introduction

29 In recent years, environmental contamination caused by toxic metals has become a
30 worldwide concern because of the potential environmental and biological problems.¹⁻⁴
31 A common heavy metal ion contaminant, chromium, is widely used in many
32 industries including tanning, electroplating, paint, textile, and metal finishing.⁵⁻⁷ Two
33 stable oxidation states of chromium, the hexavalent Cr(VI) and trivalent Cr(III) states,
34 are present in the environment. The former is known to be more toxic, teratogenic,
35 carcinogenic, mutagenic and mobile than the latter. Cr(VI) is a highly toxic ion
36 affecting aquatic life and human health at relatively low concentrations (US
37 Environmental Protection Agency (EPA), 1998). Accumulation of Cr(VI) in the
38 human body can cause either the alteration or loss of biological function. Thus, there
39 is great need to prevent further Cr(VI) contamination.⁸⁻¹⁰ At present, chemical
40 precipitation, adsorption, ion-exchange, membrane separation, reverse osmosis,
41 oxidation/reduction and electroflotation are conventional methods applied in the
42 removing Cr(VI) from wastewater.¹¹⁻¹⁵ However, high capital costs for the above
43 process limit their applicability to removing Cr(VI). Therefore, it is especially
44 important to develop a low-cost adsorbent from natural abundant materials (i.e. bio-
45 sorbents).

46 Lignin, the second most abundant renewable material next to cellulose in biomass,
47 is a very promising raw material available at low cost and low toxicity for the
48 preparation of various functional materials.^{16, 17} Due to the presence of phenolic,
49 hydroxyl, carbonyl, methoxy and aldehyde groups, lignin and its derivatives have
50 been proven to be an excellent adsorbent for removal of heavy metal ions (e.g., Hg(II),
51 Cr(VI), Cu(II), Pb(II))¹⁸⁻²⁰ and toxic dyes (e.g., Procion Blue MX-R dye, reactive dye
52 Brilliant Red HE-3B, Congo red, Eriochrome blue black R)²¹⁻²³ from industrial

53 effluents. However, after adsorption, all of the lignin and its derivatives are difficult to
54 recover from the aqueous solution using traditional separation methods filtration and
55 sedimentation.²⁴ Furthermore, commonly spent adsorbents are discarded generating
56 secondary pollution.²⁵ Thus, the difficulties encountered in regenerating lignin and its
57 derivatives limit its applications in many fields. Recently, to solve this problems, the
58 application of magnetic adsorbent technology has been received considerable
59 attention.^{26, 27} So, the preparation of magnetic lignin-based adsorbents would be a
60 good choice to solve this problem. To our knowledge, there is no report regarding the
61 removal of Cr(VI) using magnetic lignin-based adsorbents.

62 We prepared a novel diethylenetriamine modified epichlorohydrine crosslinked
63 magnetic lignin adsorbent (M–lignin–ECH–DETA) and used it to remove Cr(VI)
64 from aqueous solutions. The obtained functionalized adsorbent M–lignin–ECH–
65 DETA was characterized by SEM, FTIR, XRD, TGA and VSM. In adsorption studies,
66 the effects of pH, initial Cr(VI) concentration, contact time, temperature and
67 reusability were tested in batch experiments.

68 **2. Experimental**

69 *2.1. Chemicals*

70 Lignin was purchased from Sigma. Epichlorohydrin, diethylenetriamine, ethylene
71 glycol, ethanol, sodium acetate, sodium dodecanesulphonate, $\text{FeCl}_3 \cdot 6\text{H}_2\text{O}$, $\text{K}_2\text{Cr}_2\text{O}_7$,
72 Na_2CO_3 , NaCl, HCl and NaOH were obtained from the Sinopharm Chemical Reagent
73 Co.Ltd. (Shanghai, China). All chemicals were analytical grade and used as received
74 without further purification. An aqueous solution of Cr(VI) was prepared by
75 dissolving $\text{K}_2\text{Cr}_2\text{O}_7$ in double distilled water. A stock solution with a concentration of

76 1000 mg/L of Cr(VI) was prepared and subsequently diluted. All solutions were
77 prepared using double distilled water.

78 2.2. Preparation of Fe_3O_4

79 Fe_3O_4 was synthesized by a solvothermal reaction method.²⁸ $FeCl_3 \cdot 6H_2O$ (2.50 g)
80 was dissolved in ethylene glycol (50.0 mL) to form a clear solution. Then a sodium
81 acetate (7.50 g)–ethylene glycol (25.0 mL) solution was added dropwise into the
82 aforementioned mixture, where sodium acetate could provide elemental oxygen for
83 the formation of Fe_3O_4 and ethylene glycol served as a reductant to favor the
84 formation of Fe_3O_4 , instead of Fe_2O_3 . After vigorous stirring for 30 min, the resulting
85 homogeneous mixture was sealed in a Teflon-lined stainless steel autoclave (100 mL).
86 The autoclave was heated to 200 °C, maintained for 8 h, and allowed to cool to room
87 temperature. After magnetic separation, the precipitations were washed several
88 times with ethanol and water, and then dried at 60 °C in vacuum for 6 h.

89 2.3. Preparation of M–lignin–ECH

90 Coating of the Fe_3O_4 with lignin was achieved by a reverse phase suspension
91 method. 0.60 g Fe_3O_4 particles were dispersed in 120 mL paraffin, containing 1.50 g
92 sodium dodecanesulphonate in a three-neck flask. Then 30.0 mL of a lignin solution
93 in 12.0% (wt%) NaOH with a concentration of 10.0% w/v were added. The
94 suspension was stirred at 800 rpm with a mechanical stirrer for 30 min. Then 12.0 mL
95 epichlorohydrine solution was added and the suspension was stirred for 3 h at 60 °C.
96 The resultant magnetic lignin (M–lignin–ECH) was collected using a permanent
97 magnet and dried at 60 °C in a vacuum oven.

98 2.4. Modification of M–lignin–ECH with diethylenetriamine

99 3.0 g *M*-lignin-ECH and 75.0 mg sodium carbonate anhydrous were added into a
100 three-neck flask, and then 30.0 mL of diethylenetriamine were dropped into the
101 reaction system was kept at 70 °C for 3 h. After the reaction was completed, the
102 product (M-lignin-ECH-DETA) was isolated by magnetic separation and thoroughly
103 washed with distilled water. The precipitate was dried at 60 °C in a vacuum oven.

104 lignin-ECH-DETA was synthesized approximately following the method
105 described in 2.3 and 2.4, except for the absence of Fe₃O₄.

106 2.5. Characterization.

107 FT-IR spectra of the lignin-ECH-DETA and M-lignin-ECH-DETA were
108 recorded using a Nicolet iS50 FT-IR spectrometer in the range of 4000–400 cm⁻¹. The
109 samples were analyzed in the form of KBr pellets. Thermogravimetric analysis was
110 performed on a TG/DSC1/1100 Mettler Toledo thermogravimetric analyzer under a
111 nitrogen atmosphere from room temperature to 800 °C at a heating rate of 10 °C/ min.
112 X-ray powder diffraction (XRD) measurements were obtained by D8 Advance
113 (Bruker AXS), using CuK α radiation ($\lambda=1.5406$ Å) in the range of $2\theta=10^{\circ}$ – 70° . The
114 magnetization curve of the products were obtained using a LakeShore 7307 vibrating
115 sample magnetometer (VSM) with an applied field between –10,000 and 10,000 Oe at
116 room temperature. The samples were also analyzed with scanning electron
117 microscopy (SEM; Hitachi S–4800). The XPS study of the samples with adsorbed Cr
118 species was performed on an X-ray photoelectron spectroscopy (XPS, PHI 5000
119 VersaProbe).

120 2.6. Cr(VI) uptake experiments

121 The pH effect experiments were performed at room temperature (25 °C) by
122 adjusting the initial pH in the range of 1.0–6.0 for Cr(VI) using 0.1 M HCl. A dose of
123 40.0 mg M–lignin–ECH–DETA was mixed with 50.0 mL of 100 mg/L Cr(VI)
124 solution in several 100 mL erlenmeyer flasks. The resulting suspension was stirred for
125 12 h. The sorbent was recovered through magnetic separation after adsorption and the
126 residual solution was analyzed by the atomic absorption spectrophotometer (TAS-990,
127 Beijing Purkinje General Instrument Co. Ltd., China) to get the concentration of
128 Cr(VI).

129 Kinetic studies for Cr(VI) were conducted using 40.0 mg M–lignin–ECH–DETA in
130 50.0 mL of the adsorbate solution (100, 150 mg/L) in 100 mL Erlenmeyer flasks. The
131 suspensions were stirred at regular intervals for 10, 20, 30, 45, 60, 75, 120, 180, 240
132 min.

133 Isotherm tests were performed to determine the maximum adsorption capacity (q_{\max})
134 for Cr(VI). M–lignin–ECH–DETA (40 mg) was mixed with 50 mL solutions in 100
135 ml Erlenmeyer flasks containing adsorbates with different initial concentrations such
136 as 80, 100, 120, 150, 200, 250, 300 mg/L of Cr(VI). The suspensions were stirred for
137 12 h and the temperature was kept at 25 °C.

138 Thermodynamic parameters were measured to evaluate the effect of temperature on
139 the Cr(VI) sorption on magnetic lignin and to understand the nature of sorption. A
140 series of Erlenmeyer flasks (100 mL) containing 50.0 mL Cr(VI) solutions with initial
141 concentrations of 100 mg/L and 40.0 mg M–lignin–ECH–DETA were shaken at 25,
142 30, 35, 40 °C for 12 h.

143 The amount of adsorption (q) was defined by the following equation:

$$q_e = \frac{(c_o - c_e) \times V}{m} \quad (1)$$

144 where q_e is the amount of Cr(VI) adsorbed onto the bioadsorbents (mg/g), c_o and c_e
145 are the initial and equilibrium concentrations of Cr(VI) (mg/L), respectively. V is the
146 volume of Cr(VI) solution (L), and m is the weight of the bioadsorbents (g).

147 2.7. Regeneration experiments

148 For regeneration experiments, 0.10 g of M-lignin-ECH-DETA were loaded with
149 Cr(VI) using 125.0 mL (100 mg/L) metal ion solution at 25 °C, pH 2 and contact time
150 of 12 h. M-lignin-ECH-DETA was collected, and gently washed with distilled water
151 to remove any unabsorbed metal ions. M-lignin-ECH-DETA was then suspended
152 with 100.0 mL alkaline eluents (0.4 M NaCl+0.2 M NaOH) and stirred.

153 The regeneration efficiency was defined as:

$$\text{Regeneration efficiency (\%)} = \frac{q_n}{q_1} \times 100\% \quad (2)$$

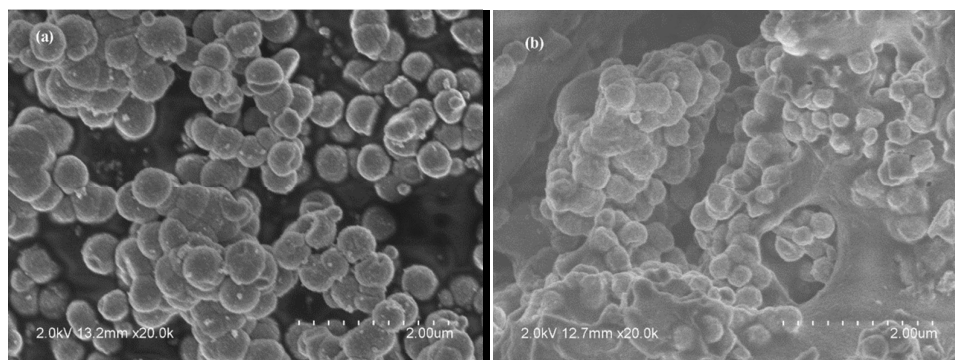
154 where q_1 is the first time the amount of Cr(VI) adsorbed onto the bioadsorbents
155 (mg/g), q_n is the n th time the amount of Cr(VI) adsorbed onto the bioadsorbents
156 (mg/g). All adsorption experiments were repeated at least twice to ensure accuracy of
157 the obtained data. The average uncertainties were <4%.

158 3. Results and discussion

159 3.1. Structure and properties of M-lignin-ECH-DETA

160 SEM images of Fe_3O_4 and M-lignin-ECH-DETA composites are presented in Fig.
161 1. It is observed that the surface of M-lignin-ECH-DETA composites was non-

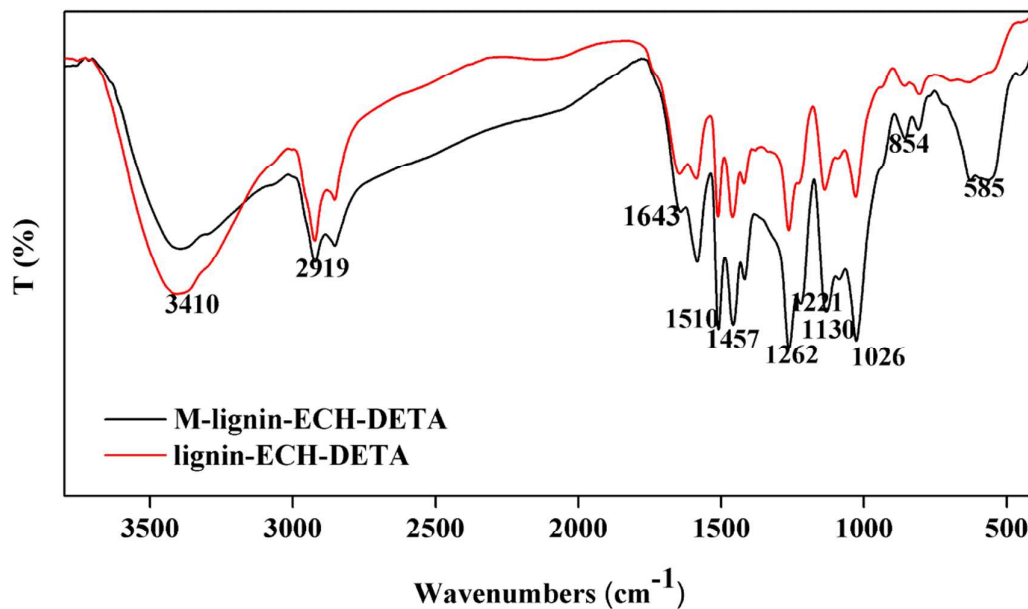
162 uniform and the interfacial adhesion that binded the Fe_3O_4 on M-lignin-ECH-DETA
163 surface was very clear.



164

165 **Fig. 1.** SEM images of (a) Fe_3O_4 and (b) M-lignin-ECH-DETA.

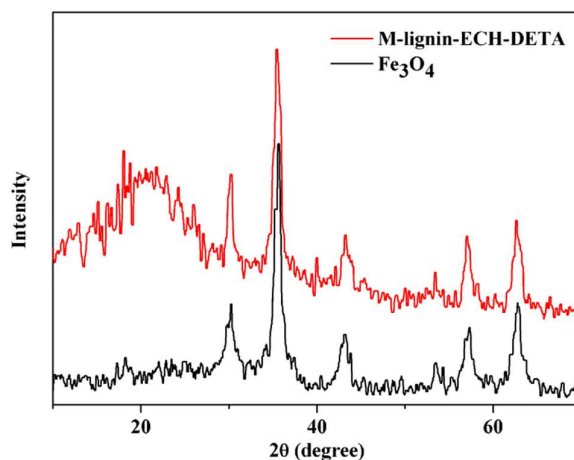
166 In the present study, FTIR spectra of M-lignin-ECH-DETA and lignin-ECH-
167 DETA are illustrated in Fig. 2. According to the reported literature,²⁹ the appearance
168 of signals at $3000\text{--}3500\text{ cm}^{-1}$ was assigned to the stretching of $-\text{OH}$, $-\text{NH}$ groups.
169 The absorption peak at 2919 cm^{-1} was attributed to C-H stretching vibration of either
170 methyl or methylene group. The peak at 1643 cm^{-1} confirmed the $-\text{NH}$ scissoring of
171 the primary amine. The peak at 1510 cm^{-1} corresponded to the aromatic skeleton
172 vibrations. The peak at 1457 cm^{-1} was originated from C-N stretching mode of amino
173 groups.²⁰ The band around 1221 cm^{-1} indicated the appearance of aromatic phenyl C-
174 O.³⁰ The biosorption band 1130 cm^{-1} was mainly due to the secondary amino
175 groups.³¹ The biosorption band 1026 cm^{-1} displayed the stretching vibration of a C-O
176 bond.³² The presence of absorption at 854 cm^{-1} for M-lignin-ECH-DETA was
177 assigned to C-H aromatic out-of-plane deformation.¹⁷ Compared to lignin-ECH-
178 DETA, the main changes to the FTIR spectrum of M-lignin-ECH-DETA was the
179 appearance of a new band at 585 cm^{-1} which was ascribed with Fe-O groups. This
180 indicated that Fe_3O_4 particles were successfully embedded in M-lignin-ECH-DETA.



181

182 **Fig. 2.** FT-IR spectra of M-lignin-ECH-DETA and lignin-ECH-DETA.

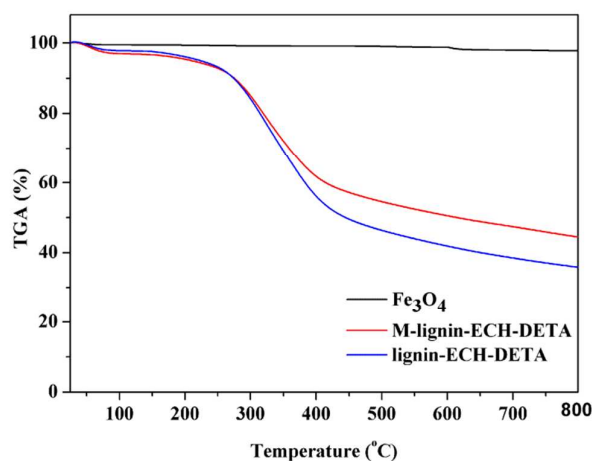
183 Fig. 3. shows the XRD patterns of Fe_3O_4 and M-lignin-ECH-DETA. Fe_3O_4 was
184 pure with a spinel structure, as can be seen from six characteristic diffraction
185 peaks($2\theta = 30.1^\circ, 35.5^\circ, 43.1^\circ, 53.4^\circ, 57.0^\circ, \text{ and } 62.5^\circ$).³³ The XRD pattern of M-
186 lignin-ECH-DETA was very similar to that of the Fe_3O_4 , implying that the crystal
187 Fe_3O_4 did not change and Fe_3O_4 have been coated in M-lignin-ECH-DETA.



188

189 **Fig. 3.** XRD pattern of Fe_3O_4 and M-lignin-ECH-DETA

190 The thermogravimetric (TG) curves obtained for the Fe_3O_4 , M-lignin-ECH-DETA,
191 lignin-ECH-DETA under N_2 atmosphere are presented in Fig. 4. The weight loss
192 could be divided into three stages for M-lignin-ECH-DETA, lignin-ECH-DETA.
193 The first stage was below 200 °C, which was ascribed to the volatilization of free
194 water. The second stage, in the range 200–500 °C, corresponded to a major weight
195 loss of the main organic component. The last stage was found from 500 to 800 °C,
196 ascribing to further decomposition of the aromatic rings of the lignin composite. The
197 thermal stability of M-lignin-ECH-DETA was higher than lignin-ECH-DETA,
198 indicating Fe_3O_4 particles have been embedded in M-lignin-ECH-DETA. It was in
199 agreement with the above-mentioned discussion. The curve for Fe_3O_4 , M-lignin-
200 ECH-DETA, lignin-ECH-DETA the residue yield was about 97.8 wt %, 44.4 wt %
201 and 35.8 wt % at 800 °C, respectively. From these numbers the mass of Fe_3O_4 in M-
202 lignin-ECH-DETA was estimated to be about 14 wt %.

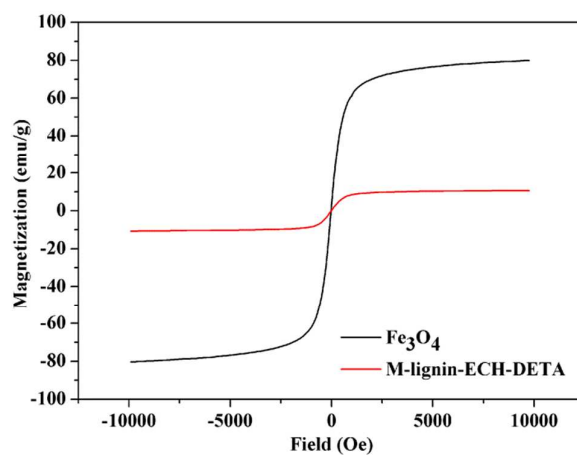


203

204 **Fig. 4.** TGA curves of Fe_3O_4 , M-lignin-ECH-DETA, lignin-ECH-DETA.

205 The magnetic hysteresis loop of Fe_3O_4 and M-lignin-ECH-DETA are
206 demonstrated in Fig. 5. As can be seen, The saturation magnetization of Fe_3O_4 and
207 M-lignin-ECH-DETA was about 79.9 and 10.6 emu/g, respectively. The result

208 indicated that M–lignin–ECH–DETA possessed a sensitive magnetic responsiveness,
209 which can be easily separated with the help of the external magnetic field.

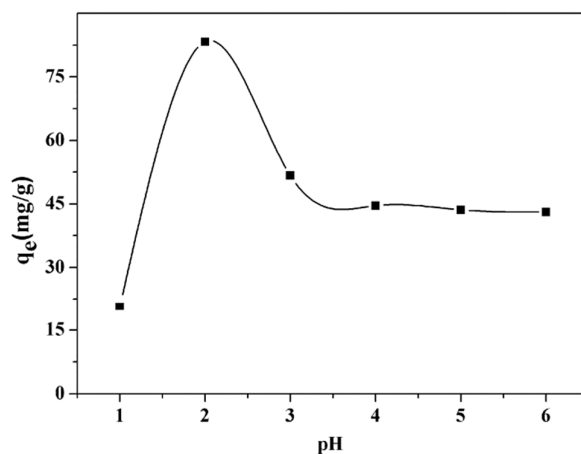


210

211 **Fig. 5.** Magnetization curves of Fe₃O₄ and M–lignin–ECH–DETA

212 *3.2. Adsorption properties*

213 *3.2.1 Effect of pH on Cr(VI) adsorption.*



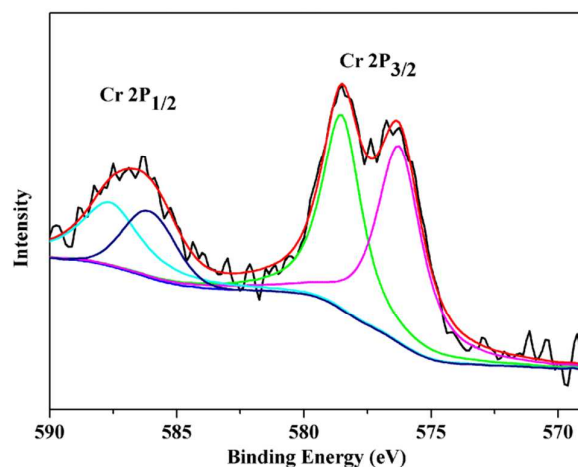
214

215 **Fig. 6.** Effect of initial pH on adsorption of Cr(VI) by M–lignin–ECH–DETA.

216 One important factor in the Cr(VI) removal was the pH value of the aqueous
217 solution, which can affect the adsorbent surface charge and Cr(VI) speciation.^{5, 34, 35}

218 The effect of pH on Cr(VI) adsorption efficiency by the M–lignin–ECH–DETA is

219 shown in Fig. 6. When pH varied from 1.0 to 2.0, the adsorption percentage of Cr(VI)
220 showed a significant increase. When pH exceeded 2.0, however, the adsorption
221 percentage of Cr(VI) decreased sharply with the rising pH value. This adsorption
222 behavior was attributed to the strong electrostatic attraction between negatively
223 charged chromium species and protonated groups located on the adsorbent surface.³⁶
224 The Cr(VI) in aqueous solution exists in various forms, such as H_2CrO_4 , HCrO_4^- ,
225 $\text{Cr}_2\text{O}_7^{2-}$, CrO_4^{2-} , etc. As the pH increases, the dominant species of Cr(VI) are H_2CrO_4
226 (pH = 1), HCrO_4^- (PH=2-4), $\text{Cr}_2\text{O}_7^{2-}$ (PH=4-6), CrO_4^{2-} (PH > 6).^{8, 35} When pH < 2.0, the
227 adsorption was low owing to the strong competition for adsorption sites between
228 H_2CrO_4 and protons.³⁷ When pH > 2.0, absorption of Cr(VI) on M-lignin-ECH-
229 DETA decreased again as the pH increased. This behaviour could be explained by
230 two reasons: first, the weakened protonation of M-lignin-ECH-DETA with rising pH
231 which reduced the electrostatic interactions between Cr(VI) species and M-lignin-
232 ECH-DETA,³⁸ second, at lower pH Cr(VI) exists as HCrO_4^- (the dominant species)
233 requiring one sorption site on the M-lignin-ECH-DETA in order for the sorption to
234 occur. However, at pH values > 4.0, the divalent forms of Cr(VI) species ($\text{Cr}_2\text{O}_7^{2-}$,
235 CrO_4^{2-}) necessitated two adjacent sorption sites on the surface of M-lignin-ECH-
236 DETA for the chromium to be firmly bound, making retention of the metal ions on the
237 surface less likely.³⁹ Furthermore, the reduction of Cr(VI) to Cr(III) may also occur in
238 the acidic condition.²⁶ To confirm this, XPS technique was employed to analyze
239 composites after adsorption. XPS spectrum is exhibited in Fig. 7. Two energy bands
240 at 586.1 eV and 576.3 eV suggested the existence of Cr(III). Therefore, according to
241 the results of XPS, we can speculate that Cr(VI) adsorbed by M-lignin-ECH-DETA
242 is partially reduced to Cr(III). Therefore, we choose pH=2 as the optimal pH value for
243 the subsequent experiments.

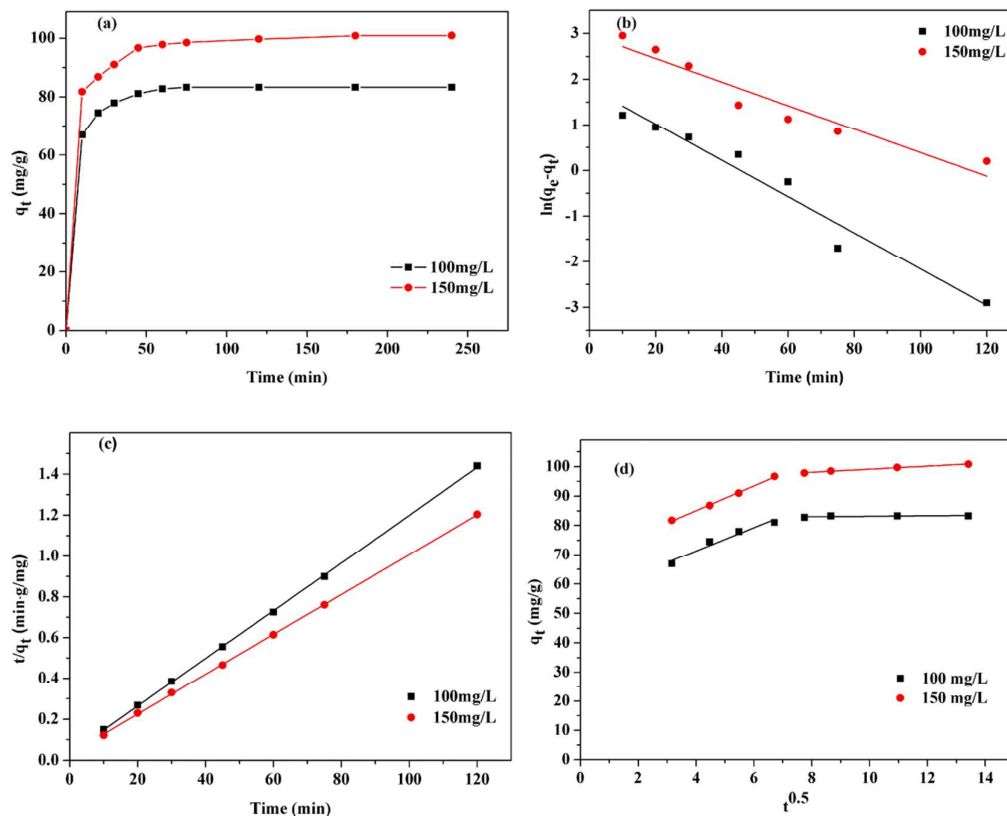


244

245 **Fig. 7.** XPS spectra of the M-lignin-ECH-DETA after Cr(VI) adsorption.

246 *3.2.2 Adsorption kinetics.*

247 Fig. 8(a) shows the effect of contact time on the adsorption of Cr(VI) ions by M-
248 lignin-ECH-DETA. It was obvious that the adsorption of Cr(VI) progressed rapidly
249 during the initial 30 minutes. Then the uptake rate decreased noticeably until after 120
250 minutes a steady state was reached. The kinetics of adsorption provided insights about
251 the mechanism of the adsorption process. In order to investigate it, the obtained
252 adsorption/time data were plotted in pseudo-first-order model, pseudo-second-order
253 and intraparticle diffusion model graphs as shown in Fig. 8(b), Fig. 8(c) and Fig. 8(d).



254

255

256 **Fig. 8.** (a) Effect of contact time on the uptake of Cr(VI) by M-lignin-ECH-DETA.
 257 (b) pseudo-first-order. (c) pseudo-second-order kinetic models. (d) intraparticle
 258 diffusion model.

259 The pseudo-first-order model equation is:

$$260 \quad \ln(q_e - q_t) = \ln q_e - K_1 t \quad (3)$$

261 The pseudo-second-order model equation is always given as:

$$\frac{t}{q_t} = \frac{1}{K_2 q_e^2} + \frac{t}{q_e} \quad (4)$$

262 The intraparticle diffusion model is represented as follow:

$$263 \quad q_t = K_i t^{0.5} + C \quad (5)$$

264 where q_e and q_t (mg/g) are the amount of Cr(VI) adsorbed on M-lignin-ECH-
 265 DETA at equilibrium and at a given time t , respectively. K_1 is rate constant (min^{-1}) of
 266 pseudo-first-order model. K_2 (g/(mg min)) is the adsorption rate constant of pseudo-
 267 second-order model. K_i is the intraparticle diffusion. C is the thickness of the
 268 boundary layer.

269 **Table 1.** Kinetic parameters obtained through pseudo-first-order and pseudo-second-
 270 order for the adsorption of Cr(VI) onto M-lignin-ECH-DETA at initial concentration
 271 of 100 and 150 mg/L.

Concentration Cr(VI)(mg/L)	pseudo-first-order			
	$q_{e,\text{exp}}$ (mg/g)	$q_{e1,\text{cal}}$ (mg/g)	K_1	R^2
100	83.33	6.13	0.0397	0.952
150	100.89	19.48	0.0258	0.908
	pseudo-second-order			
	$q_{e,\text{exp}}$ (mg/g)	$q_{e2,\text{cal}}$ (mg/g)	K_2	R^2
100	83.33	85.54	0.0044	0.999
150	100.89	102.35	0.0032	0.999

272

273 The fitting parameters of adsorption kinetics are listed in Table 1. The correlation
 274 coefficients of the pseudo-second-order model (R^2) were higher than that of the
 275 pseudo-first-order model (R^2). Moreover, compared with pseudo-first-order model,
 276 adsorption values ($q_{e2,\text{cal}}$) calculated by the pseudo-second order model were closer to
 277 the experimental results ($q_{e,\text{exp}}$). This indicated that the adsorption process of Cr(VI)
 278 on M-lignin-ECH-DETA could be considered as a pseudo-second-order model
 279 process. This implied that the Cr(VI) uptake process was chemisorptions. Fig. 8(d)
 280 shows the plot of the amount of Cr(VI) adsorbed (q_t) versus the square root of time

281 $(t^{0.5})$. It can be seen that the adsorption data are fitted by two separate straight lines.
282 This revealed that the adsorption of Cr(VI) on M–lignin–ECH–DETA is a process
283 involving external diffusion and final intraparticle diffusion.^{26, 27, 40}

284 3.2.3 Adsorption isotherm

285 For interpretation of the interaction between the adsorbent and adsorbate, Langmuir,
286 Freundlich and Temkin adsorption isotherm models were employed to analyze
287 experimental data and describe the equilibrium of adsorption.

288 Langmuir equation is represented as follows:

$$\frac{1}{q_e} = \frac{1}{q_m} + \frac{1}{K_L q_m c_e} \quad (6)$$

289 the Freundlich isotherm is depicted by the following equation:

$$\ln q_e = \ln K_F + \frac{1}{n} \ln c_e \quad (7)$$

290

291 Temkin can be presented by the following equation:

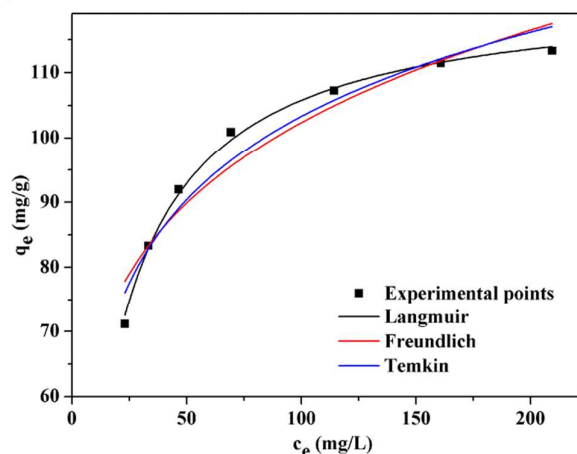
$$q_e = B \ln A + B \ln c_e \quad (8)$$

293 where q_e and c_e are the amount of Cr(VI) ions adsorbed (mg/g) at equilibrium and the
294 adsorbate concentration in solution (mg/L), respectively. q_m (mg/g) and K_L (mL/g) are
295 the Langmuir constants related to the saturated sorption capacity and sorption energy,
296 respectively. $K_F [(mg/g)(L/mg)^{1/n}]$ is Freundlich constant which indicate the capacity
297 of the adsorption. n is the heterogeneity factor. A is the equilibrium binding

298 constant corresponding to the maximum binding energy and constant B is related to
 299 the heat of adsorption. The Cr(VI) adsorption isotherms for M–lignin–ECH–DETA
 300 are presented in Fig. 9. and isotherm parameters are summarized in Table 2.

301 **Table 2.** Parameters of the Langmuir isotherm, Freundlich isotherm, and Temkin
 302 models for Cr(VI) biosorption onto M–lignin–ECH–DETA.

Freundlich isotherm			Langmuir isotherm			Temkin		
K_F	n	R^2	q_m	K_L	R^2	A	B	R^2
43.28	5.35	0.913	123	0.063	0.996	2.60	18.58	0.944



303

304 **Fig. 9.** Isotherm curves of Cr(VI) adsorption on M–lignin–ECH–DETA.

305 As could be seen from Fig. 9, the adsorption of Cr(VI) would increase with the
 306 initial concentration. However, above a certain concentration, the adsorption capacity
 307 of Cr(VI) trended toward steady state, saturated, values. Langmuir, Freundlich and
 308 Temkin adsorption isotherm model fits show that the correlation coefficient of
 309 Langmuir isotherm ($R^2=0.996$) is higher than that of Freundlich isotherm ($R^2=0.913$)
 310 and Temkin isotherm ($R^2=0.944$). Hence, the adsorption isotherms are described well
 311 by the Langmuir isotherm models. The calculated maximum Cr(VI) uptake q_m is 123
 312 mg/g. In other words, the adsorbed material M–lignin–ECH–DETA forms a

313 monolayer on the surface with a finite number of identical sites that are
 314 homogeneously distributed across the adsorbent surface.

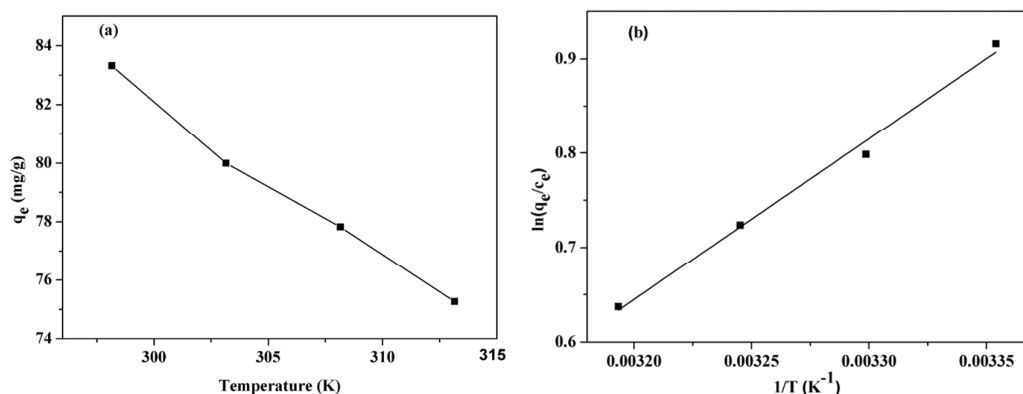
315 3.2.4 Adsorption thermodynamics

316 Fig. 10 shows the adsorption of Cr(VI) biosorption onto M–lignin–ECH–DETA at
 317 different temperatures. The results found that the adsorption capacity decreased with
 318 increasing temperature. The thermodynamic parameters (ΔG° , ΔS° and ΔH°) were
 319 calculated using the following equation:

$$\Delta G = -RT \ln(q_e/c_e) \quad (9)$$

$$\ln\left(\frac{q_e}{c_e}\right) = \frac{\Delta S}{R} - \frac{\Delta H}{RT} \quad (10)$$

320 where q_e and c_e are the amount of Cr(VI) ions adsorbed (mg/g) at equilibrium and the
 321 adsorbate concentration in solution (mg/L), respectively. R is the universal gas
 322 constant (8.134 J/(K·mol)), T is the temperature in Kelvin. The thermodynamic
 323 parameters for the adsorption of Cr(VI) are listed in Table 3.



324

325 **Fig. 10.** (a) Effect of temperature on the uptake of Cr(VI) using M–lignin–ECH–
 326 DETA. (b) Thermodynamic plot of $\ln(q_e/c_e)$ vs. $1/T$.

327 Table 3. Thermodynamic parameters for the adsorption of Cr(VI) using M–lignin–
328 ECH–DETA.

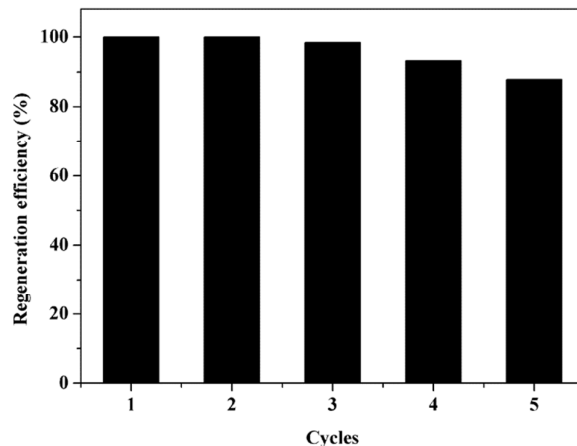
ΔH° (kJ/mol)	ΔS° (J/(k mol))	ΔG° (kJ/mol)			
		298K	303K	308K	313K
-14.1513	-39.9213	-2.2706	-2.0126	-1.8542	-1.6594

329

330 The negative values of ΔG° indicated the adsorption is spontaneous and feasibility of
331 the adsorption of Cr(VI) on the M–lignin–ECH–DETA. The magnitude of the value
332 of ΔG° decreased from -2.2706 to -1.6594 kJ/mol in the temperature range of 298–
333 313 K, suggesting the adsorption is not favorable at higher temperatures.⁴⁰ The
334 negative value of ΔH° implied that the adsorption of Cr(VI) onto M–lignin–ECH–
335 DETA was exothermic in nature and the adsorption of Cr(VI) was more effective at
336 lower temperature. The negative value of ΔS° reflected decreasing randomness at the
337 solid/solution interface during the adsorption process.⁴¹

338 3.2.5 Regeneration experiments

339 The recycling of adsorbents plays an important role in evaluating the potential
340 applicability of adsorbents. After adsorption of Cr(VI) onto the M–lignin–ECH–
341 DETA, desorption experiments have been carried out using 0.4 M NaCl and 0.2 M
342 NaOH. Then the regenerated M–lignin–ECH–DETA was reused to adsorb Cr(VI).
343 The results are shown in Fig. 11. From this figure can be seen that the adsorption
344 capacity was reduced with the number of regeneration times. In addition, the
345 regeneration efficiency of the M–lignin–ECH–DETA after five times still could reach
346 more than 87 %. Therefore, M–lignin–ECH–DETA could be utilized repeatedly for
347 the treatment of Cr(VI) effluents.



348

349 **Fig. 11.** Effect of recycling M-lignin-ECH-DETA on Cr(VI) adsorption.

350 4. Conclusions

351 In this study, a novel magnetic lignin composite was prepared and acted as a
352 promising adsorbent for the adsorption of Cr(VI). The results showed that the optimal
353 pH value was pH 2.0. Adsorption kinetics could be described well by a pseudo-
354 second-order model. A Langmuir model represented the adsorption isotherm well and
355 the maximum adsorption amount of Cr(VI) was calculated to be 123 mg/g. The
356 obtained thermodynamic parameters revealed that the adsorption of Cr(VI) onto the
357 adsorbent was an exothermic and spontaneous process. Additionally, magnetic lignin
358 composite could be separated well using the magnetic properties of the composite.
359 The composite showed good reusability losing only 13% of its capacity after 5 cycles.
360 All these results demonstrated that the material is promising as sorbent in reducing
361 pollution of Cr(VI) effluents.

362 5. Acknowledgements

363 The authors are grateful to the National Natural Science Foundation of China
364 (21206057), the Natural Science Foundation of Jiangsu Province, China (BK2012118)

365 and (BK2012547), and MOE & SAFEA for the 111 Project (B13025) for financial
366 support.

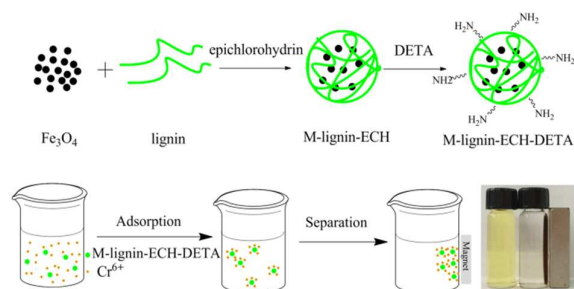
367 6. Reference

- 368 1. L. Zhou, Y. Wang, Z. Liu and Q. Huang, *J. Hazard. Mater.* 2009, **161**, 995-
369 1002.
- 370 2. K. Z. Elwakeel, *Desalination*. 2010, **250**, 105-112.
- 371 3. A. Zafar, S. A. Eqani, N. Bostan, A. Cincinelli, F. Tahir, S. T. Shah, A.
372 Hussain, A. Alamdar, Q. Huang, S. Peng and H. Shen, *Environ. Geochem.*
373 *Hlth.* 2014, DOI 10.1007/s10653-014-9666-8.
- 374 4. Z. Wu, Y. Du, H. Xue, Y. Wu and B. Zhou, *Neurobiol. Aging*. 2012, **33**,
375 199.e1-199.e12.
- 376 5. W. Liu, J. Zhang, C. Zhang and L. Ren, *Chem. Eng. J.* 2012, **189-190**, 295-
377 302.
- 378 6. Y. G. Abou El-Reash, M. Otto, I. M. Kenawy and A. M. Ouf, *Int. J. Biol.*
379 *Macromol.* 2011, **49**, 513-522.
- 380 7. Y. Chen, H. Xu, S. Wang and L. Kang, *RSC Adv.* 2014, **4**, 17805.
- 381 8. Q. Q. Zhong, Q. Y. Yue, Q. Li, B. Y. Gao and X. Xu, *Carbohydr. Polym.*
382 2014, **111**, 788-796.
- 383 9. T. Norseth, *Br. J. Ind. Med.* 1986, **43**, 649-651.
- 384 10. S. Langard, *Sci. Total. Environ.* 1988, **71**, 341-350.
- 385 11. L. Zhou, Z. Zhang, W. Jiang, W. Guo, H. H. Ngo, X. Meng, J. Fan, J. Zhao
386 and S. Xia, *Biofouling*. 2014, **30**, 105-114.
- 387 12. J. Liu, C. Wang, J. Shi, H. Liu and Y. Tong, *J. Hazard. Mater.* 2009, **163**,
388 370-375.

- 389 13. H.-y. Xu, Z.-h. Yang, G.-m. Zeng, Y.-l. Luo, J. Huang, L.-k. Wang, P.-p. Song
390 and X. Mo, *Chem. Eng. J.* 2014, **239**, 132-140.
- 391 14. C. E. Barrera-Diaz, V. Lugo-Lugo and B. Bilyeu, *J. Hazard. Mater.* 2012,
392 **223-224**, 1-12.
- 393 15. G. Barassi, A. Valdes, C. Araneda, C. Basualto, J. Sapag, C. Tapia and F.
394 Valenzuela, *J. Hazard. Mater.*, 2009, **172**, 262-268.
- 395 16. A. Brandt, J. Gräsvik, J. P. Hallett and T. Welton, *Green Chem.* 2013, **15**, 550.
- 396 17. F. Monteil-Rivera, M. Phuong, M. Ye, A. Halasz and J. Hawari, *Ind. Crop.*
397 *Prod.* 2013, **41**, 356-364.
- 398 18. Y. Zhou, J. P. Zhang, X. G. Luo and X. Lin, *J. Appl. Polym. Sci.* 2014, DOI:
399 10.1002/APP.40749
- 400 19. V. Nair, A. Panigrahy and R. Vinu, *Chem. Eng. J.* 2014, **254**, 491-502.
- 401 20. Y. Ge, Z. Li, Y. Kong, Q. Song and K. Wang, *J. Ind. Eng. Chem.* 2014, **20**,
402 4429-4436.
- 403 21. M. A. Adebayo, L. D. Prola, E. C. Lima, M. J. Puchana-Rosero, R. Cataluna,
404 C. Saucier, C. S. Umpierrez, J. C. Vaggetti, L. G. da Silva and R. Ruggiero, *J.*
405 *Hazard. Mater.* 2014, **268**, 43-50.
- 406 22. D. Suteu, T. Malutan and D. Bilba, *Desalination.* 2010, **255**, 84-90.
- 407 23. X. Wang, Y. Zhang, C. Hao, X. Dai, Z. Zhou and N. Si, *RSC Adv.* 2014, **4**,
408 28156-28164.
- 409 24. D. H. Reddy and S. M. Lee, *Adv. Colloid Interfac.*, 2013, **201**, 68-93.
- 410 25. Y. M. Hao, C. Man and Z. B. Hu, *J. Hazard. Mater.*, 2010, **184**, 392-399.
- 411 26. Y.-J. Jiang, X.-Y. Yu, T. Luo, Y. Jia, J.-H. Liu and X.-J. Huang, *J. Chem. Eng.*
412 *Data*, 2013, **58**, 3142-3149.

- 413 27. C. Gao, X.-Y. Yu, T. Luo, Y. Jia, B. Sun, J.-H. Liu and X.-J. Huang, *J. Mater.*
414 *Chem. A*, 2014, **2**, 2119-2128.
- 415 28. S. Wang, Y.-Y. Zhai, Q. Gao, W.-J. Luo, H. Xia and C.-G. Zhou, *J. Chem.*
416 *Eng. Data*. 2014, **59**, 39-51.
- 417 29. X. Yu, S. Tong, M. Ge, L. Wu, J. Zuo, C. Cao and W. Song, *Carbohydr.*
418 *Polym.* 2013, **92**, 380-387.
- 419 30. P. Manara, A. Zabaniotou, C. Vanderghem and A. Richel, *Catal. Today*. 2014,
420 **223**, 25-34.
- 421 31. T. S. Anirudhan and T. A. Rauf, *J. Ind. Eng. Chem.* 2013, **19**, 1659-1667.
- 422 32. C. Yuwei and W. Jianlong, *Chem. Eng. J.* 2011, **168**, 286-292.
- 423 33. J.-s. Wang, R.-t. Peng, J.-h. Yang, Y.-c. Liu and X.-j. Hu, *Carbohydr. Polym.*,
424 2011, **84**, 1169-1175.
- 425 34. X. Sun, L. Yang, Q. Li, Z. Liu, T. Dong and H. Liu, *Chem. Eng. J.* 2015, **262**,
426 101-108.
- 427 35. N. N. Thinh, P. T. Hanh, T. T. Ha le, N. Anh le, T. V. Hoang, V. D. Hoang, H.
428 Dang le, N. V. Khoi and T. D. Lam, *Mater. Sci. Eng., C*. 2013, **33**, 1214-1218.
- 429 36. W. Jin, Z. Zhang, G. Wu, R. Tolba and A. Chen, *RSC Adv.* 2014, **4**, 27843-
430 27849.
- 431 37. X. J. Hu, J. S. Wang, Y. G. Liu, X. Li, G. M. Zeng, Z. L. Bao, X. X. Zeng, A.
432 W. Chen and F. Long, *J. Hazard. Mater.* 2011, **185**, 306-314.
- 433 38. X. Jin, M. Jiang, J. Du and Z. Chen, *J. Ind. Eng. Chem.* 2014, **20**, 3025-3032.
- 434 39. A. M. Yusof and N. A. Malek, *J. Hazard. Mater.* 2009, **162**, 1019-1024.
- 435 40. L. Zhou, J. Liu and Z. Liu, *J. Hazard. Mater.* 2009, **172**, 439-446.
- 436 41. A. H. Qusti, *J. Ind. Eng. Chem.* 2014, **20**, 3394-3399.
- 437

Graphical Abstract



Novel magnetic lignin composite remove Cr(VI)